
Research Article: New Research | Cognition and Behavior

Aerobic glycolysis is required for spatial memory acquisition but not memory retrieval in mice

Richard A. Harris¹, Asad Lone¹, Heeseung Lim², Francisco Martinez³, Ariel K. Frame¹, Timothy J. Scholl^{2,3,4} and Robert C. Cumming¹

¹*Department of Biology, University of Western Ontario, London, Ontario, Canada*

²*Department of Medical Biophysics, University of Western Ontario, London, Ontario, Canada*

³*Robarts Research Institute, University of Western Ontario, London, Ontario, Canada*

⁴*Ontario Institute for Cancer Research, Toronto, Ontario, Canada*

<https://doi.org/10.1523/ENEURO.0389-18.2019>

Received: 3 October 2018

Revised: 23 January 2019

Accepted: 26 January 2019

Published: 11 February 2019

R.A.H., T.J.S., and R.C.C. designed research; R.A.H., A.L., H.L., F.M., and A.F. performed research; R.A.H., A.L., and R.C.C. analyzed data; R.A.H., A.L., and R.C.C. wrote the paper.

Funding: <http://doi.org/10.13039/501100000038>Gouvernement du Canada | Natural Sciences and Engineering Research Council of Canada (NSERC) 355803-2013 06338-2017

Funding: Canadian Consortium on Neurodegeneration in Aging 137794

Funding: <http://doi.org/10.13039/501100000096>Scottish Rite Charitable Foundation of Canada (SRCFC) 11103

Funding: <http://doi.org/10.13039/501100000196>Canada Foundation for Innovation (CFI) 22167

The authors declare no competing financial interests.

Natural Sciences and Engineering Research Council of Canada 355803-2013 (RCC) and 06338-2017 (TJS), Scottish Rite Charitable Foundation 11103 (RCC), Canada Foundation for Innovation 22167 (RCC), Canadian Consortium on Neurodegeneration in Aging 137794 (RCC & RB)

R.A.H. and A.L. Denotes equal author contribution

Correspondence should be addressed to Robert C. Cumming, rcummin5@uwo.ca

Cite as: eNeuro 2019; 10.1523/ENEURO.0389-18.2019

Alerts: Sign up at www.eneuro.org/alerts to receive customized email alerts when the fully formatted version of this article is published.

Accepted manuscripts are peer-reviewed but have not been through the copyediting, formatting, or proofreading process.

Copyright © 2019 Harris et al.

This is an open-access article distributed under the terms of the Creative Commons Attribution 4.0 International license, which permits unrestricted use, distribution and reproduction in any medium provided that the original work is properly attributed.

1 **Aerobic glycolysis is required for spatial memory acquisition but not memory**
2 **retrieval in mice**

3 Abbreviated Title: Dichloroacetate impairs spatial learning in mice

4

5 **Richard A. Harris*¹, Asad Lone*¹, Heeseung Lim², Francisco Martinez³, Ariel K. Frame¹,**
6 **Timothy J. Scholl^{2,3,4}, and Robert C. Cumming¹**

7 *Denotes equal author contribution

8

9 ¹Department of Biology, University of Western Ontario, London, Ontario, Canada;

10 ²Department of Medical Biophysics, University of Western Ontario, London, Ontario, Canada

11 ³Robarts Research Institute, University of Western Ontario, London, Ontario, Canada

12 ⁴Ontario Institute for Cancer Research, Toronto, Ontario, Canada

13

14 RH, TS, and RC Designed Research; RH, AL, HL, FM, and AF Performed Research, RH and

15 AL Analyzed data, RH, AL, and RC Wrote the paper.

16

17 To whom correspondence should be addressed: Robert C. Cumming, Department of Biology,

18 University of Western Ontario, 1151 Richmond Street North, London, Ontario Canada N6A

19 5B7, Tel.:(519) 661-2111; Fax: (519) 661-3935; E-mail: rcummin5@uwo.ca

20

21 Number of Figures: 4

22 Number of Tables: 0

23 Number of Multimedia: 0

24 Number of words for Abstract: 243

25 Number of words for Significance: 119

26 Number of words for Introduction: 460

27 Number of words for Discussion: 1,702

28 Acknowledgments: This work was supported in part by the Natural Sciences and Engineering
29 Research Council of Canada 355803-2013 (RCC) and 06338-2017 (TJS), Scottish Rite
30 Charitable Foundation 11103 (RCC), Canada Foundation for Innovation 22167 (RCC), Canadian
31 Consortium on Neurodegeneration in Aging 137794 (RCC)

32

33 Conflict of Interest: The authors declare no competing financial interests.

34

35 Funding sources: Natural Sciences and Engineering Research Council of Canada 355803-2013
36 (RCC) and 06338-2017 (TJS), Scottish Rite Charitable Foundation 11103 (RCC), Canada
37 Foundation for Innovation 22167 (RCC), Canadian Consortium on Neurodegeneration in Aging
38 137794 (RCC & RB)

39

40 **ABSTRACT**

41 The consolidation of newly formed memories and their retrieval are energetically demanding
42 processes. Aerobic glycolysis (AG), also known as the Warburg effect, consists of the production
43 of lactate from glucose in the presence of oxygen. The astrocyte neuron lactate shuttle hypothesis
44 posits that astrocytes process glucose by AG to generate lactate, which is used as a fuel source
45 within neurons to maintain synaptic activity. Studies in mice have demonstrated that lactate
46 transport between astrocytes and neurons is required for long-term memory formation, yet the role
47 of lactate production in memory acquisition and retrieval has not previously been explored. Here,
48 we examined the effect of dichloroacetic acid (DCA), a chemical inhibitor of lactate production,
49 on spatial learning and memory in mice using the Morris Water Maze (MWM). *In vivo*
50 hyperpolarized ¹³C-pyruvate magnetic resonance spectroscopy revealed decreased conversion of
51 pyruvate to lactate in the mouse brain following DCA administration, concomitant with a reduction
52 in phosphorylation of pyruvate dehydrogenase (PDH). DCA exposure before each training session
53 in the MWM impaired learning, which subsequently resulted in impaired memory during the probe
54 trial. In contrast, mice that underwent training without DCA exposure, but received a single DCA
55 injection before the probe trial exhibited normal memory. Our findings indicate that AG plays a
56 key role during memory acquisition but is less important for retrieval of established memories.
57 Thus, activation of AG may be important for learning-dependent synaptic plasticity rather than the
58 activation of signaling cascades required for memory retrieval.

59

60 **SIGNIFICANCE**

61 Neuronal activation is an energetically demanding process. The brain is mainly fueled by glucose,
62 yet a substantial portion of this metabolite is converted to lactate despite the presence of adequate
63 oxygen, a phenomenon known as aerobic glycolysis (AG). The transport of lactate between
64 astrocytes and neurons is key for learning and memory, yet the role of lactate production in these

65 processes is poorly understood. Here we report that administration of dichloroacetate (DCA), a
66 chemical inhibitor of AG, attenuates conversion of pyruvate to lactate in the brains of mice. DCA
67 exposure impaired spatial learning but had no effect on the retrieval of an established memory.
68 These observations suggest that lactate production may be required for memory acquisition but
69 not retrieval.

70

71 INTRODUCTION

72 Glucose is the primary fuel source within the human brain (Mergenthaler et al., 2013) and can be
73 processed by various metabolic pathways to produce energy. Under normal oxygen tension,
74 glucose is typically broken down in the cytosol to pyruvate, which then enters the mitochondria
75 and undergoes oxidative decarboxylation by pyruvate dehydrogenase (PDH) to produce acetyl-
76 CoA. Acetyl-CoA provides carbon atoms for the tricarboxylic acid (TCA) cycle leading to the
77 production of NADH and FADH₂, ultimately generating 32–36 ATP molecules by oxidative
78 phosphorylation. Under hypoxic conditions, pyruvate is preferentially converted to lactate by
79 lactate dehydrogenase (LDHA) to produce 2 ATP molecules in a process known as anaerobic
80 glycolysis. However, a third way to process glucose, termed aerobic glycolysis (AG), occurs when
81 glucose is processed to generate lactate despite normal oxygen tension. Under resting conditions,
82 AG accounts for 10-15% of glucose consumed in the human brain and increases to up to 40%
83 following neuronal activation (Raichle et al., 1970; Boyle et al., 1994; Powers et al., 2007; Madsen
84 et al., 1998, 1999). Recent evidence has implicated lactate, the end product of AG, in the regulation
85 of synaptic plasticity and gene expression changes associated with learning and memory (Goyal
86 et al., 2014; Shannon et al., 2016; Suzuki et al., 2011; Yang et al., 2014). Astrocytes are believed
87 to be the primary cell type in the central nervous system that use AG to generate lactate, which is
88 subsequently transported to neurons to meet their high energy needs (Magistretti and Allaman,
89 2018). Astrocytic glycogen can also be mobilized via glycogenolysis to generate glucose for

90 subsequent processing by AG to generate lactate (Brown et al., 2004). Numerous studies in rodents
91 have shown that inhibition of astrocytic glycogenolysis or lactate transport results in compromised
92 learning and memory (Magistretti and Allaman, 2018). However, the effect of AG inhibition on
93 cognitive processes has yet to be examined.

94

95 Dichloroacetate (DCA) is a blood brain barrier (BBB) permeable chemical that selectively inhibits
96 pyruvate dehydrogenase kinase (PDK) (Kato et al., 2008). Phosphorylation of PDH by PDK results
97 in a strong suppression of PDH activity, thereby favouring AG and lactate production (Kato et al.,
98 2008). Based on its ability to inhibit PDK and promote optimal mitochondrial PDH activity, DCA
99 has been used clinically to lower lactate levels in the blood and cerebral spinal fluid of patients
100 with congenital lactic acidosis (Stacpoole et al., 2003). In this study we examined the effect of
101 DCA-mediated inhibition of AG on spatial learning and memory in mice. Exposure to DCA readily
102 prevented the phosphorylation of PDH and reduced the conversion of pyruvate to lactate within
103 the brain. Moreover, DCA administration significantly impaired spatial learning but had no effect
104 on the recall of established memories, suggesting that AG may play a role in memory acquisition
105 but not retrieval.

106

107 **MATERIALS AND METHODS**

108 *Animals*

109 Male C57BL/6J mice (RRID:IMSR_JAX:000664) were housed in groups under a 12 hour
110 light/dark cycle with *ad libitum* access to base chow (2018 Teklad global diet; Envigo) and tested
111 at 9 months of age. All animal procedures were performed in compliance with the Canadian
112 Council on Animal Care guidelines under an animal protocol approved by the University of
113 Western Ontario animal care committee.

114

115 *Hyperpolarized ^{13}C -pyruvate magnetic resonance spectroscopy*

116 Images were acquired using a multinuclear-capable 3.0-Tesla MRI system (General Electric
117 Healthcare Discovery MR750 3.0 T, Milwaukee WI, U.S.A.). A custom-built dual-tuned ^1H - ^{13}C
118 solenoid radiofrequency coil was used to facilitate inherent registration of ^1H and ^{13}C images.
119 Buffered hyperpolarized [$1\text{-}^{13}\text{C}$]pyruvate (95% enriched ^{13}C content, Sigma Aldrich, Miamisburg
120 OH, U.S.A.) solution was produced using dynamic nuclear polarization (HyperSense, Oxford
121 Instruments, Abingdon, UK). The hyperpolarized solution had a final concentration of 150mM
122 pyruvate with pH 7.4 at 37°C and ~10% polarization producing a signal enhancement factor of >
123 10,000 for MRSI. The *in vivo* spin-lattice relaxation time was ~45s. The imaging session consisted
124 of fast imaging employing steady-state free-precession ^1H image acquisition (FIESTA) and
125 hyperpolarized ^{13}C MRSI. Prior to ^{13}C MRSI, FIESTA images were acquired with the following
126 imaging parameters: 30 x 30mm field of view (FOV), 0.2mm isotropic in-plane resolution, 0.4mm
127 slice thickness, repetition time (TR) = 10.3ms, echo time (TE) = 5.2ms, bandwidth = 12.58Hz, and
128 phase cycling = 8. For hyperpolarized ^{13}C MRSI, a ~0.3 ml bolus of the hyperpolarized [$1\text{-}^{13}\text{C}$]
129 pyruvate buffered solution was injected over 10 seconds via a tail vein catheter and allowed to
130 circulate for 15 seconds for cell uptake and conversion of the ^{13}C -labeled pyruvate prior to
131 imaging. 2D MRSI was performed using a free induction decay chemical shift pulse sequence
132 (FID-CSI) with the following parameters: 30 x 30mm FOV, 2.5-mm isotropic in-plane resolution,
133 slice thickness = 10~15mm, TR = 80ms, spectral width = 5000 Hz and number of points = 256.
134 Total MRSI acquisition time was ~12 seconds. DCA (Sigma Aldrich, Oakville ON) was freshly
135 prepared at a concentration of 40mg/mL in sterile saline and neutralized to pH 7.4 \pm 0.1 using
136 NaOH. Mice were given 30 minutes to recover following hyperpolarized ^{13}C -pyruvate injection
137 before injection of DCA at 200mg/kg via tail vein catheter. Mice were then given an additional 30
138 minutes to recover, followed by another bolus of hyperpolarized ^{13}C -pyruvate vial a tail vein
139 catheter. Mice immediately underwent a second ^{13}C MRSI imaging session as previously

140 described. Intravenous injection of DCA, as opposed to intraperitoneal injection used in learning
141 and memory testing (described below), was necessary due to the technical requirement of
142 maintaining exact head position during all stages of MRS imaging.

143

144 *Western blot analysis of brain extracts*

145 Mice were sedated in a CO₂ chamber and then immediately perfused with Dulbecco's phosphate
146 buffered saline (DPBS), pH 7.4 containing 2mM leupeptin, 0.1mM pepstatin A, 100mM EDTA,
147 1mM PMSF, and 0.5mM sodium orthovanadate. The brain was removed, and the frontal cortex of
148 the right hemisphere was homogenized in an extraction buffer containing 50 mM Tris pH 7.5, 2%
149 SDS, and protease and phosphatase inhibitors. Protein extracts were resolved by 10% SDS PAGE,
150 and electroblotted onto PVDF membrane (Bio-Rad). Membranes were probed with the following
151 antibodies: PDK1 (Enzo Life Sciences Cat# KAP-PK112D, RRID:AB_1193509), PDH-E1 α
152 (pSer²³²) (Millipore Cat# AP1063, RRID:AB_10616070), PDH-E1 α (Abcam Cat# ab110330,
153 RRID:AB_10858459), and β -actin (Cell Signaling Technology Cat# 3700, RRID:AB_2242334).
154 Bands were detected using Luminata Forte chemiluminescence substrate (EMD Millipore) and
155 imaged using a Chemidoc XRS System (Bio-Rad, Mississauga, ON). Densitometric analysis was
156 performed using Quantity One 1-D Analysis Software (Bio-Rad, RRID:SCR_014280).

157

158 *Water maze apparatus*

159 The MWM consisted of a uniformly white circular pool with a diameter of 48" and height of 30"
160 (San Diego Instruments) and was divided into four fictive quadrants. The pool was filled with
161 water and maintained at a temperature of 24°C using a 300W submersible aquarium heater
162 (Aqueon). Spatial visual cues in the form of different shaped cardboard pictures were placed on
163 the walls surrounding the water tank. Mice were first submitted to a single habituation session of

164 three trials, in which the mouse was placed on circular plastic platform (diameter 10.16 cm)
165 positioned 1 cm below the surface of the water in the center of the pool for 15 seconds. Following
166 habituation, mice were trained for 4 consecutive days, with 4 trials per day to find the location of
167 the circular platform located in the center of the target quadrant. The release point for the first trial
168 of the day corresponded to the cardinal directions (i.e. North, East, South, West), rotating
169 clockwise with each new training day. For each subsequent trial session on a given day, mice were
170 released into the water at a position that was on quarter turn clockwise from the previous trial
171 release point. A trial lasted until either the mouse found the platform or until 90 seconds had
172 elapsed, at which point the mouse was gently guided to the platform and left there for 15 seconds
173 before it was removed. Following each trial mice were towed dry and placed in their home cage
174 for an inter-trial interval of 10 minutes to allow recovery and ensure consistency of timing between
175 trials. On the fifth day, the platform was removed and the mouse was released in the center of the
176 tank, and given 60 seconds to attempt to find the missing platform. A second probe trial was
177 performed one week later, using the same procedure as the first probe trial. A flag trial was also
178 performed in which the platform was placed back into the water within the quadrant that was
179 opposite to that used during the training trials and a small red plastic pole was inserted into the
180 platform so as to create a visual cue. The mouse was released in the center of the tank and given
181 90 seconds to find the location of the platform. Visual data was collected and analyzed using ANY-
182 maze v4.98 (ANY-maze, RRID:SCR_014289). Animals were injected intraperitoneally with
183 either saline or DCA (Sigma) at a dose of 200mg/kg. One cohort of mice were injected with either
184 saline or DCA 30 minutes prior to the start of each training session while a second cohort of mice
185 underwent normal training but received either a saline or DCA injection 30 minutes before the
186 probe trial.

187

188

189 *Statistical analysis*

190 A Welch's paired t-test was used to analyze the difference between the ratio of lactate to pyruvate
191 for before and after DCA injection. A Welch's unpaired t-test was used to analyze band
192 densitometry and memory performance for saline- and DCA-injected mice. A two-way ANOVA
193 with repeated measures was used to analyze the difference between latency to the platform, path
194 length, and mean speed for saline- and DCA-injected mice during training. Statistical evaluation
195 was performed using RStudio v0.97.551 (RStudio, RRID:SCR_000432).

196

197 **RESULTS**

198 **DCA reduces conversion of pyruvate to lactate in the mouse brain.** In order to test if DCA
199 was a suitable compound for manipulating AG and lactate production in the brain, mice were
200 analyzed using hyperpolarized ^{13}C -pyruvate magnetic resonance spectroscopy 30 minutes before,
201 and 30 minutes after, injection of DCA (200mg/kg) via an intravenous tail-vein catheter (**Fig. 1A**).
202 ^{13}C -pyruvate spectra were collected within individual voxels throughout the whole brain (**Fig. 1B**)
203 and combined to calculate the ratio of lactate-to-pyruvate as an indication of pyruvate conversion
204 to lactate in the mouse brain before and after DCA injection (**Fig. 1C**). The observed lactate-to-
205 pyruvate metabolite ratio within the brain was significantly reduced from 0.144 ± 0.034 (mean \pm
206 SEM) before DCA exposure to 0.056 ± 0.016 after DCA administration ($t_{(1,10)} = 2.753$, $p < 0.05$)
207 (**Fig. 1D**). Thus, DCA administration reduces lactate production from pyruvate in the mouse brain
208 30 minutes after infusion, indicating that it is a suitable compound for inhibiting AG.

209

210 **DCA injection reduces the phosphorylation of PDH in the frontal cortex and hippocampus.**

211 To confirm that DCA exerts an effect on the brain regions related to spatial learning and memory,
212 the phosphorylated form of PDH was measured in brain extracts from the frontal cortex and
213 hippocampus 30 minutes after intraperitoneal injection of DCA. DCA administration caused a

214 significant decrease in PDH phosphorylation levels in both the frontal cortex ($t_{(1,10)} = 13.78$, $p <$
215 0.001) and hippocampus ($t_{(1,14)} = 4.493$, $p < 0.001$) compared to saline-injected mice (**Fig. 2**). A
216 significant decrease in PDK1 expression was also observed in the frontal cortex of DCA-injected
217 mice ($t_{(1,10)} = 2.837$, $p < 0.05$). These results are in accordance with previous observations that DCA
218 readily crosses the blood brain barrier and targets AG by increasing PDH activity (Kato et al.,
219 2008).

220

221 **DCA administration causes impairment in spatial learning.** To determine if AG is required
222 for spatial learning, a task that is dependent upon communication between the hippocampus and
223 frontal cortex, mice were injected intraperitoneally with DCA 30 minutes prior to each training
224 session for the Morris water maze (MWM) task. Several measures were recorded for each training
225 day, including the latency to find the platform, the total path length, and the mean speed (**Fig. 3A-**
226 **C**). DCA administration resulted in a significant reduction in learning, as reflected by the increased
227 latency time to find the platform ($F_{(1,12)} = 9.83$, $p < 0.01$) and increased path length ($F_{(1,12)} = 12.84$,
228 $p < 0.01$), compared to saline injected mice. There was no significant difference in mean speed
229 between the two groups ($F_{(1,12)} = 2.93$, $p = 0.11$). Mice exposed to DCA during training
230 subsequently exhibited a reduced ability to locate the platform during the probe trial as visualized
231 by a trace analysis of the swim path in a heat map (**Fig. 3D**). DCA-injected mice also displayed a
232 significantly reduced percent time spent in the correct quadrant ($t_{(1,12)} = 2.21$, $p < 0.05$) and a
233 reduction in the number of platform entries ($t_{(1,12)} = 3.71$, $p < 0.05$) compared to saline-injected
234 mice, yet displayed no difference in total distance covered during the trial ($t_{(1,12)} = 0.01$, $p = 0.99$)
235 (**Fig. 3E-G**). A second probe trial, performed one week later, revealed that DCA exposure during
236 training impaired long-term memory, as indicated by a significant decrease in number of platform
237 crosses ($t_{(1,12)} = 3.25$, $p < 0.01$) compared to saline-treated controls (**Fig 3H**). Thus, DCA injection

238 caused an impairment in learning that subsequently weakened memory association with the
239 location of the platform both 24 hours and 7-days after training.

240

241 **DCA administration does not interfere with memory recall.** We next asked whether AG is
242 required for spatial memory recall. Mice underwent 4 days of training in the MWM and were then
243 injected intraperitoneally with DCA 30 minutes prior to the probe trial on the fifth day (**Fig. 4A**).
244 DCA-injected mice showed no difference in memory performance from saline-injected mice, as
245 demonstrated visually by a trace analysis of the swim path in a heat map (**Fig. 4B**). The total
246 distance covered in the probe trial revealed no significant difference between saline- and DCA-
247 injected mice ($t_{(1,16)} = 0.80, p = 0.43$) (**Fig. 4C**). In addition, no significant differences in memory
248 performance was observed, as indicated by the percent of time spent in the correct quadrant ($t_{(1,16)}$
249 $= 0.52, p = 0.31$) and the total number of platform entries ($t_{(1,16)} = 0.77, p = 0.45$) (**Fig. 4D,E**). In
250 order to confirm that DCA had no adverse effect on vision, a flag trial was performed which
251 demonstrated that saline- and DCA-injected mice exhibited similar times to find the flag ($t_{(1,16)} =$
252 $0.16, p = 0.44$) (**Fig. 4F**). These findings indicate that AG is not explicitly required for spatial
253 memory retrieval. In addition, DCA injection had no adverse effects on swimming performance
254 or visual acuity.

255

256

257 **DISCUSSION**

258 The role of glycogenolysis and lactate transport in learning and memory has been extensively
259 studied (Magistretti and Allaman, 2018). Rats undergoing training during an inhibitory avoidance
260 (IA) test exhibit a transient elevation of hippocampal lactate levels, measured by *in vivo*
261 microdialysis, that is completely abolished by bilateral injection of the glycogenolysis inhibitor
262 1,4-dideoxy-1,4-imino-D-arabinitol (DAB) into the hippocampus (Suzuki et al., 2011). In a

263 separate study, DAB injection in the rat hippocampus 5 minutes prior to behavioural testing
264 significantly impaired spatial working memory in a 4-arm spontaneous alternation task (Newman
265 et al., 2017). Moreover, DAB-mediated impairment of spatial working memory was rescued by
266 hippocampal injection of lactate (Newman et al., 2011). Chemical or genetic inhibition of
267 monocarboxylate transporters (MCTs) that shuttle lactate in the brain also impairs IA and spatial
268 working memory (Newman et al., 2011; Suzuki et al., 2011). Lactate derived from astrocytic
269 glycogenolysis, and its subsequent transport to neurons, was shown to mediate hippocampal long-
270 term potentiation (LTP), and induce learning-dependent molecular changes, including increased
271 expression of immediate early genes such as activity-regulated cytoskeletal protein (Arc), proto-
272 oncogene c-Fos, early growth response 1 (Egr1) and phosphorylation of cAMP response element-
273 binding protein (pCREB) and cofilin (p-cofilin) (Suzuki et al., 2011; Yang et al., 2014).
274 Collectively, these observations provide strong support for the astrocyte neuron lactate shuttle
275 model in which glucose, either directly or supplied via astrocytic glycogenolysis, is processed by
276 AG within astrocytes to generate lactate that is then transported to neurons to fuel the high energy
277 demands associated with the cellular and molecular changes underlying memory formation and
278 storage. However, the precise role of task-based activation of AG in memory acquisition and
279 retrieval is poorly defined.

280

281 Several studies have demonstrated a task-associated decrease in extracellular glucose and a
282 concurrent rise in extracellular lactate in the hippocampus during spatial memory processing
283 (McNay et al., 2006, 2000; Newman et al., 2017). In addition, genes involved in AG, including
284 LDHA and PDK, show increased hippocampal expression following IA learning, suggesting that
285 induction of enzymes that promote lactate production may be required for memory acquisition
286 (Tadi et al., 2015). Rats also exhibit increased AG in the amygdala during IA training and memory
287 testing (Sandusky et al., 2013). Interestingly, a marked increase in extracellular pyruvate was

288 observed in the amygdala during IA training whereas a significant drop in pyruvate was observed
289 during memory testing (Sandusky et al., 2013). These observations prompted the authors to
290 speculate that memory acquisition relies predominately on AG whereas memory retrieval places a
291 higher demand on oxidative metabolism. Our findings are in accordance with this theory as
292 discussed below.

293

294 In this study we demonstrate for the first time that systemic DCA administration causes a decline
295 in lactate production from pyruvate with a concomitant reduction in PDH phosphorylation in the
296 frontal cortex and hippocampus; brain regions critical for spatial memory formation. In support of
297 previous studies, we also show evidence that DCA can readily cross the BBB and inhibit PDK
298 activity, thereby lowering PDH phosphorylation and reducing lactate production (Abemayor et al.,
299 1984; Stacpoole et al., 2003). DCA injection before each training trial resulted in impaired
300 learning, as reflected by the increased latency and increased total path length required to find the
301 platform in the MWM. In addition, DCA-mediated inhibition of AG during training resulted in a
302 reduced ability to locate the platform during subsequent probe trials. Although DCA exposure may
303 potentially cause non-specific effects (disorientation, perceptual and motivational alterations), this
304 is unlikely because we did not detect a significant difference in the mean speed during training, or
305 a decrease in the ability to find the flag during the probe trial following DCA injection.
306 Interestingly, a single DCA injection before the probe trial had no effect on memory performance
307 in mice that had already undergone regular training, indicating that AG is not explicitly required
308 for memory retrieval. In light of these observations, we theorize that the transient increase in AG
309 is required for the initial phases of learning, but not retrieval of established memories.

310

311 In support of this theory, several studies have shown that AG is quickly up-regulated in response
312 to neural stimulation and can account for up to 40% of the glucose consumed by active brain

313 regions (Fox et al., 1988; Madsen et al., 1999, 1998). In a recent study, PET scans of humans
314 before and after a visual–motor adaptation task revealed that the left Brodmann area 44 played a
315 key role in task performance that correlated strongly with an increase in AG in the same brain
316 region (Shannon et al., 2016). Thus, elevated AG may arise to support the increased energetic
317 demand in brain regions engaged in specific tasks. Moreover, AG plays a critical role in synaptic
318 plasticity by enabling the synthesis of biosynthetic building blocks derived from glycolytic
319 intermediates to support processes such as cytoskeletal rearrangements, lipid synthesis, protein
320 trafficking and increased gene expression (Bas-Orth et al., 2017; Bauernfeind et al., 2013; Yang
321 et al., 2009). The spatial distribution of AG in the human brain also correlates with the expression
322 of developmental and neotenus genes, strongly implicating AG in supporting new synapse
323 formation and growth (Goyal et al., 2014). Indeed, recent studies have shown that exposure of
324 mouse primary cortical neurons to lactate stimulates the expression of synaptic plasticity-related
325 genes including *Arc*, *c-Fos*, *Bdnf* and *Egr1* through an NMDA receptor dependent mechanism
326 (Margineanu et al., 2018; Yang et al., 2014).

327

328 Whether AG is up-regulated directly in astrocytes, neurons, or both is currently a contentious issue
329 (Dienel, 2012). Uptake of the glucose analogue 6-deoxy-N-(7-nitrobenz-2-oxa-1,3-diazol-4-yl)-
330 aminoglucose (6-NBDG), as assessed by *in vivo* two-photon imaging, revealed preferential uptake
331 in astrocytes during activation of the somatosensory cortex in mice (Chuquet et al., 2010). Two-
332 photon imaging of mouse hippocampal and cerebellar brain slices demonstrated that the transport
333 and metabolism of the fluorescent glucose analog 2-NBDG is higher in astrocytes than in neurons
334 located in their vicinity (Jakoby et al., 2014). In addition, confocal imaging of mouse primary
335 cultures transfected with a genetically encoded FRET glucose biosensor revealed that glucose
336 uptake is faster in astrocytes than neurons (Jakoby et al., 2014). However, several recent reports
337 have provided evidence suggesting that glucose may also be taken up by neurons. Two-photon

338 imaging analysis, using a near-infrared fluorophore, IRDye 800CW, conjugated to 2-deoxyglucose
339 (2DG-IR), revealed that 2DG-IR was taken up preferentially by neurons in awake behaving mice
340 and that sensory stimulation leads to a pronounced increase in neuronal, but not astrocytic, 2DG-
341 IR uptake (Lundgaard et al., 2015). However, it should be noted that 2DG-IR is likely internalized
342 as a macromolecular complex with the glucose transporter GLUT1 by endocytosis and may not
343 adequately reflect physiological glucose uptake (Kovar et al., 2009). A separate study, using
344 metabolic biosensors in hippocampal slices and brains of awake mice, revealed that neuronal
345 stimulation is dependent on increased glucose consumption directly by neurons, not astrocytic-
346 derived lactate (Díaz-García et al., 2017). Intrahippocampal injection of indinavir, a selective
347 chemical inhibitor of the neuronal GLUT4 glucose transporter, before IA training in rats resulted
348 in impaired learning, whereas inhibition of glucose transport after training had no effect on
349 memory retrieval (Pearson-Leary and McNay, 2016). The discrepancies between astrocytic and
350 neuronal uptake of glucose in the aforementioned studies may be attributed to a number of factors
351 including regional variation in glucose metabolism, the task-dependent nature of glucose uptake,
352 and limitations when using glucose analogues and biosensors to measure glucose uptake and
353 processing. Regardless, we propose that the transient elevation of neuronal glycolysis may act as
354 a “first responder” to meet the increased energy needs of stimulated neurons due to the fact that
355 glycolysis can generate ATP at a much faster rate than mitochondrial oxidative phosphorylation,
356 while lactate production may spur expression of immediate early genes involved in LTP.

357

358 Recent studies have shown that the glycolytic enzymes PDK1 and LDHA are primarily expressed
359 within neurons of the frontal cortex and hippocampus of wild type and transgenic Alzheimer’s
360 disease mice (Harris et al., 2016; Zhang et al., 2018). Interestingly, it was recently shown that
361 induction of synaptic activity promotes increased neuronal glucose uptake and expression of
362 glycolytic genes (Bas-Orth et al., 2017; Segarra-Mondejar et al., 2018). Moreover, synaptic

363 activity triggered increases in glucose metabolism and promotes the generation of lipid precursors
364 required for cell membrane enlargement during neurite outgrowth (Segarra-Mondejar et al., 2018).
365 It is possible that AG occurs in neurons during the initial phases of learning to promote structural
366 synaptic remodeling within memory engram neurons. Once memory acquisition and synaptic
367 remodeling has occurred, then mitochondrial oxidative phosphorylation may play a prominent role
368 in ensuring that sufficient ATP production occurs to maintain established connections associated
369 with memory recall. It is our intention that these findings will spur future studies to further dissect
370 apart the role of either astrocytic or neuronal AG in various paradigms of learning and memory.

371

372 While our findings suggest that AG is required for memory acquisition, we could not determine
373 the role of AG on memory consolidation due to the limitations of the experimental design used in
374 this study. Memory consolidation has typically been evaluated using classical behavioural assays
375 with rapid acquisition such as the passive-avoidance task (Lorenzini et al., 1996) or fear
376 conditioning (Schafe et al., 1999). It is generally easier to differentiate post-training events, such
377 as memory consolidation, from learning when the duration of the acquisition phase is short. The
378 multiple training sessions used in the MWM over 4 days may result in memory traces that are
379 reactivated and reconsolidated during each learning session, possibly obscuring events associated
380 with the initial consolidation of a spatial memory (Florian and Roulet, 2004). However, several
381 studies have made use of a massed training protocol for the MWM in which mice are submitted to
382 four consecutive trial sessions within a 70-90 minute period followed by a probe trial 24 hours
383 later (Florian and Roulet, 2004; Stein et al., 2014; Villain et al., 2016). The 1 day protocol can
384 expose deficits in early consolidation after the training sessions without the complication of
385 overlapping learning and consolidation processes during multi-day training protocols (Stein et al.,
386 2014). In future studies, it would be of interest to use the 1-day MWM training protocol and

387 administer DCA after the condensed training sessions to determine if inhibition of AG also
388 interferes with the early events associated with memory consolidation.

389

390 REFERENCES

- 391 Abemayor E, Kovachich GB, Haugaard N (1984) Effects of dichloroacetate on brain pyruvate
392 dehydrogenase. *J Neurochem* 42:38–42.
- 393 Bas-Orth C, Tan Y-W, Lau D, Bading H (2017) Synaptic Activity Drives a Genomic Program
394 That Promotes a Neuronal Warburg Effect. *J Biol Chem* 292:5183–5194.
- 395 Bauernfeind AL, Barks SK, Duka T, Grossman LI, Hof PR, Sherwood CC (2013) Aerobic
396 glycolysis in the primate brain: reconsidering the implications for growth and maintenance.
397 *Brain Struct Funct.*
- 398 Boyle PJ, Scott JC, Krentz AJ, Nagy RJ, Comstock E, Hoffman C (1994) Diminished brain
399 glucose metabolism is a significant determinant for falling rates of systemic glucose
400 utilization during sleep in normal humans. *J Clin Invest* 93:529–535.
- 401 Brown AM, Baltan Tekkök S, Ransom BR (2004) Energy transfer from astrocytes to axons: the
402 role of CNS glycogen. *Neurochem Int* 45:529–536.
- 403 Chuquet J, Quilichini P, Nimchinsky EA, Buzsáki G (2010) Predominant enhancement of
404 glucose uptake in astrocytes versus neurons during activation of the somatosensory cortex. *J*
405 *Neurosci* 30: 15298-15303
- 406 Dienel GA (2012) Brain lactate metabolism: the discoveries and the controversies. *J Cereb Blood*
407 *Flow Metab* 32:1107–1138.
- 408 Florian C, Rouillet P (2004) Hippocampal CA3-region is crucial for acquisition and memory
409 consolidation in Morris water maze task in mice. *Behav Brain Res* 154:365–374.

- 410 Fox PT, Raichle ME, Mintun MA, Dence C (1988) Nonoxidative glucose consumption during
411 focal physiologic neural activity. *Science* 241:462–464.
- 412 Goyal MS, Hawrylycz M, Miller JA, Snyder AZ, Raichle ME (2014) Aerobic glycolysis in the
413 human brain is associated with development and neotenus gene expression. *Cell Metab*
414 19:49–57.
- 415 Harris RA, Tindale L, Lone A, Singh O, Macauley SL, Stanley M, Holtzman DM, Bartha R,
416 Cumming RC (2016) Aerobic Glycolysis in the Frontal Cortex Correlates with Memory
417 Performance in Wild-Type Mice But Not the APP/PS1 Mouse Model of Cerebral
418 Amyloidosis. *J Neurosci Off J Soc Neurosci* 36:1871–1878.
- 419 Jackoby P, Schmidt E, Ruminot I, Gutiérrez R, Barros LF, Deitmer JW (2014) Higher transport
420 and metabolism of glucose in astrocytes compared with neurons: a multiphoton study of
421 hippocampal and cerebellar tissue slices. *Cereb Cortex* 24:222–231.
- 422 Kato M, Wynn RM, Chuang JL, Tso S-C, Machius M, Li J, Chuang DT (2008) Structural basis
423 for inactivation of the human pyruvate dehydrogenase complex by phosphorylation: role of
424 disordered phosphorylation loops. *Struct Lond Engl* 1993 16:1849–1859.
- 425 Kovar JL, Volcheck W, Sevick-Muraca E, Simpson MA, Olive DM (2009) Characterization and
426 performance of a near infrared 2-deoxyglucose optical imaging agent for mouse cancer
427 models. *Anal Biochem* 384:254–262.
- 428 Lorenzini CA, Baldi E, Bucherelli C, Sacchetti B, Tassoni G (1996) Role of dorsal hippocampus
429 in acquisition, consolidation and retrieval of rat's passive avoidance response: a tetrodotoxin
430 functional inactivation study. *Brain Res* 730:32–39.
- 431 Lundgaard I, Li B, Xie L, Kang H, Sanggaard S, Haswell JDR, Sun W, Goldman S, Blekot S,
432 Nielsen M, Takano T, Deane R, Nedergaard M (2015) Direct neuronal glucose uptake heralds
433 activity-dependent increases in cerebral metabolism. *Nat Commun* 6:6807.

- 434 Madsen PL, Cruz NF, Sokoloff L, Dienel GA (1999) Cerebral oxygen/glucose ratio is low
435 during sensory stimulation and rises above normal during recovery: excess glucose
436 consumption during stimulation is not accounted for by lactate efflux from or accumulation in
437 brain tissue. *J Cereb Blood Flow Metab Off J Int Soc Cereb Blood Flow Metab* 19:393–400.
- 438 Madsen PL, Linde R, Hasselbalch SG, Paulson OB, Lassen NA (1998) Activation-induced
439 resetting of cerebral oxygen and glucose uptake in the rat. *J Cereb Blood Flow Metab Off J*
440 *Int Soc Cereb Blood Flow Metab* 18:742–748.
- 441 Magistretti PJ, Allaman I (2018) Lactate in the brain: from metabolic end-product to signalling
442 molecule. *Nat Rev Neurosci* 19:235–249.
- 443 Margineanu MB, Mahmood H, Fiumelli H, Magistretti PJ (2018) L-Lactate Regulates the
444 Expression of Synaptic Plasticity and Neuroprotection Genes in Cortical Neurons: A
445 Transcriptome Analysis. *Front Mol Neurosci* 11:375.
- 446 McNay EC, Fries TM, Gold PE (2000) Decreases in rat extracellular hippocampal glucose
447 concentration associated with cognitive demand during a spatial task. *Proc Natl Acad Sci U S*
448 *A* 97:2881–2885.
- 449 McNay EC, Williamson A, McCrimmon RJ, Sherwin RS (2006) Cognitive and neural
450 hippocampal effects of long-term moderate recurrent hypoglycemia. *Diabetes* 55:1088–1095.
- 451 Mergenthaler P, Lindauer U, Dienel GA, Meisel A (2013) Sugar for the brain: the role of glucose
452 in physiological and pathological brain function. *Trends Neurosci* 36:587–597.
- 453 Newman LA, Korol DL, Gold PE (2011) Lactate Produced by Glycogenolysis in Astrocytes
454 Regulates Memory Processing. *PLoS ONE* 6:e28427.
- 455 Newman LA, Scavuzzo CJ, Gold PE, Korol DL (2017) Training-induced elevations in
456 extracellular lactate in hippocampus and striatum: Dissociations by cognitive strategy and
457 type of reward. *Neurobiol Learn Mem* 137:142–153.

- 458 Pearson-Leary J, McNay EC (2016) Novel Roles for the Insulin-Regulated Glucose Transporter-
459 4 in Hippocampally Dependent Memory. *J Neurosci Off J Soc Neurosci* 36:11851–11864.
- 460 Powers WJ, Videen TO, Markham J, McGee-Minnich L, Antenor-Dorsey JV, Hershey T,
461 Perlmutter JS (2007) Selective defect of in vivo glycolysis in early Huntington’s disease
462 striatum. *Proc Natl Acad Sci U S A* 104:2945–2949.
- 463 Raichle ME, Posner JB, Plum F (1970) Cerebral blood flow during and after hyperventilation.
464 *Arch Neurol* 23:394–403.
- 465 Sandusky LA, Flint RW, McNay EC (2013) Elevated glucose metabolism in the amygdala
466 during an inhibitory avoidance task. *Behav Brain Res* 245:83–87.
- 467 Schafe GE, Nadel NV, Sullivan GM, Harris A, LeDoux JE (1999) Memory consolidation for
468 contextual and auditory fear conditioning is dependent on protein synthesis, PKA, and MAP
469 kinase. *Learn Mem Cold Spring Harb N* 6:97–110.
- 470 Segarra-Mondejar M, Casellas-Díaz S, Ramiro-Pareta M, Müller-Sánchez C, Martorell-Riera A,
471 Hermelo I, Reina M, Aragonés J, Martínez-Estrada OM, Soriano FX (2018) Synaptic activity-
472 induced glycolysis facilitates membrane lipid provision and neurite outgrowth. *EMBO J* 37.
- 473 Shannon BJ, Vaishnavi SN, Vlassenko AG, Shimony JS, Rutlin J, Raichle ME (2016) Brain
474 aerobic glycolysis and motor adaptation learning. *Proc Natl Acad Sci* 113:E3782–E3791.
- 475 Stacpoole PW, Nagaraja NV, Hutson AD (2003) Efficacy of dichloroacetate as a lactate-
476 lowering drug. *J Clin Pharmacol* 43:683–691.
- 477 Stein IS, Donaldson MS, Hell JW (2014) CaMKII binding to GluN2B is important for massed
478 spatial learning in the Morris water maze. *F1000Research* 3:193.
- 479 Suzuki A, Stern SA, Bozdagi O, Huntley GW, Walker RH, Magistretti PJ, Alberini CM (2011)
480 Astrocyte-neuron lactate transport is required for long-term memory formation. *Cell* 144:810–
481 823.

- 482 Tadi M, Allaman I, Lengacher S, Grenningloh G, Magistretti PJ (2015) Learning-Induced Gene
483 Expression in the Hippocampus Reveals a Role of Neuron -Astrocyte Metabolic Coupling in
484 Long Term Memory. PLOS ONE 10:e0141568.
- 485 Villain H, Florian C, Rouillet P (2016) HDAC inhibition promotes both initial consolidation and
486 reconsolidation of spatial memory in mice. Sci Rep 6:27015.
- 487 Yang G, Pan F, Gan W-B (2009) Stably maintained dendritic spines are associated with lifelong
488 memories. Nature 462:920–924.
- 489 Yang J, Ruchti E, Petit J-M, Jourdain P, Grenningloh G, Allaman I, Magistretti PJ (2014)
490 Lactate promotes plasticity gene expression by potentiating NMDA signaling in neurons. Proc
491 Natl Acad Sci 111:12228–12233.
- 492 Zhang M, Cheng X, Dang R, Zhang W, Zhang J, Yao Z (2018) Lactate Deficit in an Alzheimer
493 Disease Mouse Model: The Relationship With Neuronal Damage. J Neuropathol Exp Neurol
494 77:1163-1176

495
496

497 LEGENDS

498 **Figure 1. Hyperpolarized ^{13}C -pyruvate magnetic resonance spectroscopic imaging reveals**
499 **decline in lactate following DCA administration. (A)** Injection and imaging regime of 9-month-
500 old mice using hyperpolarized MRSI of [$1\text{-}^{13}\text{C}$] pyruvate to measure the conversion of pyruvate to
501 lactate. Mice were imaged after the first ^{13}C -pyruvate injection (Before) and 30 minutes later were
502 then injected with DCA (200 mg/kg). Following a 30-minute recovery time, another injection of
503 ^{13}C -pyruvate and imaging was performed (After). **(B)** ^1H MRI image of the brain in the coronal
504 field overlaid with MRSI voxels containing spectra of ^{13}C -labeled pyruvate and lactate (yellow).
505 **(C)** Conversion of pyruvate to lactate was measured as a ratio of the observed lactate peak to

506 pyruvate peak from before DCA injection (blue line) and after (red dashed line). A pyruvate
507 hydrate peak was also recorded. **(D)** DCA injection reduces the ratio of lactate to pyruvate in the
508 mouse brain ($P = 0.04$). Data shown are mean \pm SEM, $n = 4$.

509

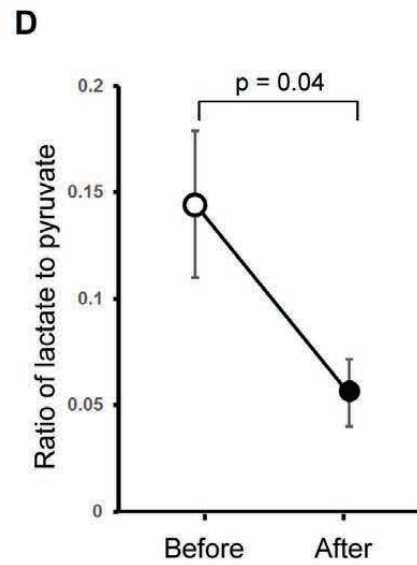
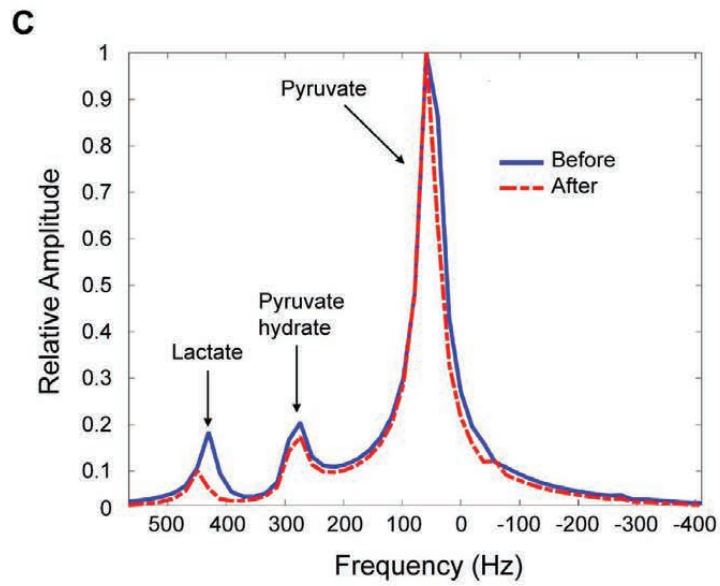
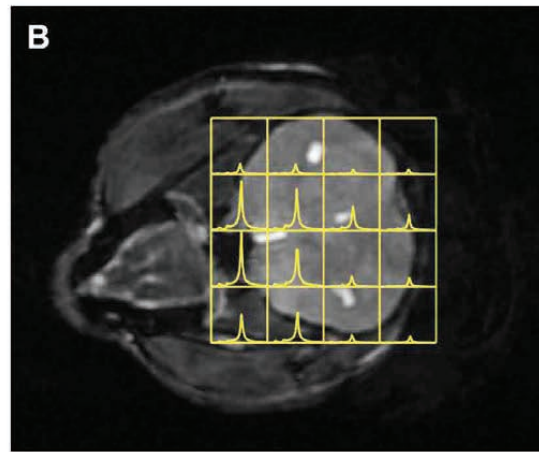
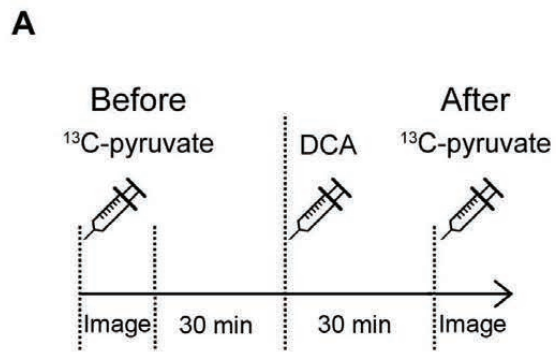
510 **Figure 2. DCA injection reduces the phosphorylation of PDH in the frontal cortex and**
511 **hippocampus.** Western blot analysis (left) was performed on extracts from the frontal cortex **(A)**
512 and the hippocampus **(B)** of mice i.p. injected with either saline or DCA (200mg/kg) 30 minutes
513 prior to euthanization. Densitometric analysis of western blots (right) revealed significantly lower
514 PDH phosphorylation in DCA treated mice relative to saline injected mice ($*P < 0.05$, $***P < 0.001$,
515 $n = 6$ and 6 , respectively, for extracts from the frontal cortex of saline- and DCA-injected mice,
516 and $n = 7$ and 7 , respectively, for extracts from the hippocampus of saline- and DCA-injected
517 mice). Band densities were standardized to β -actin controls. Data shown are mean \pm SEM.

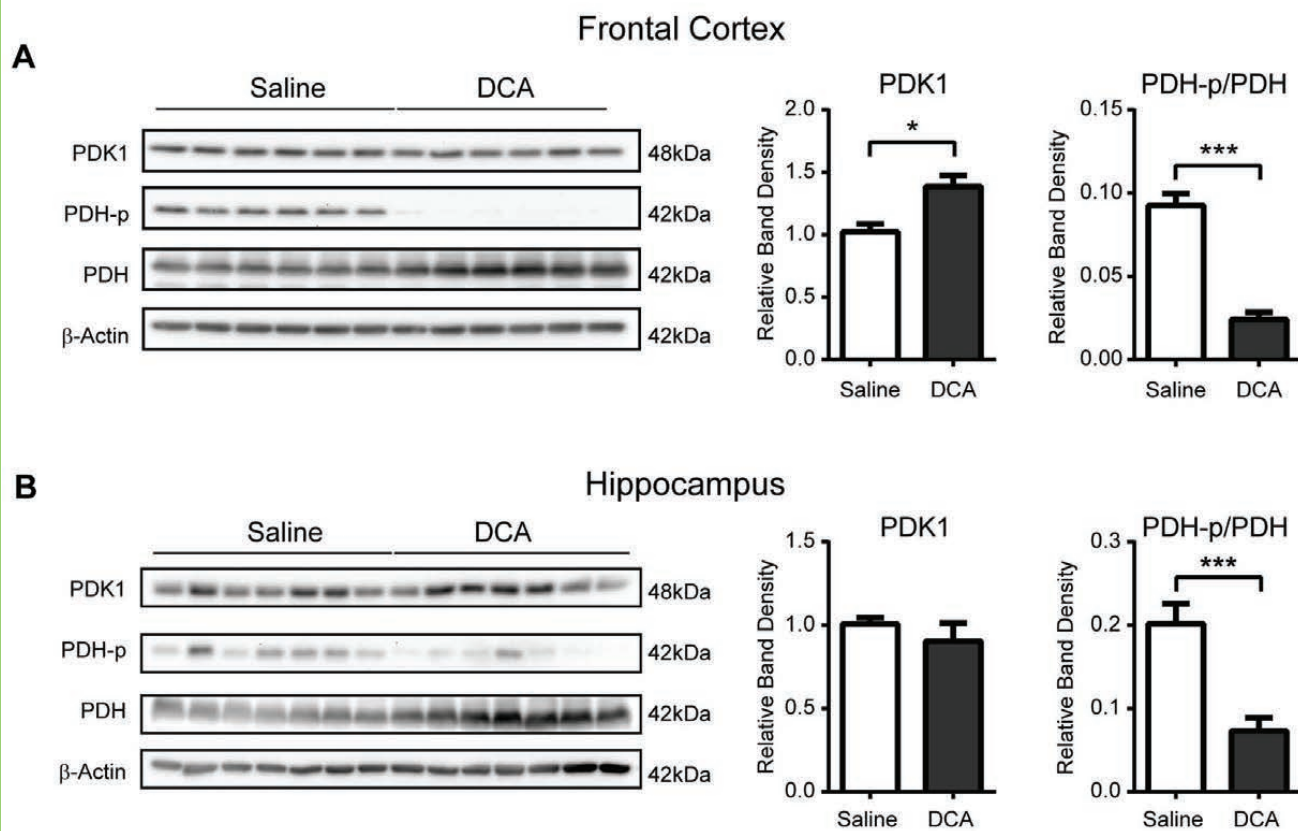
518

519 **Figure 3. DCA administration causes impairment in spatial learning.** Mice were i.p. injected
520 with saline or DCA (200mg/kg) 30 minutes before each day of training and allowed to find the
521 location of a hidden platform in the NW quadrant. **(A)** The latency to find the platform, **(B)** the
522 total path length, and **(C)** the mean speed was recorded on each training day. On day 5, a probe
523 trial was performed without DCA injection and mice were allowed to swim for 60 seconds **(D-G)**.
524 **(D)** The swim path for each group of mice was compiled into heat map representations.
525 Measurements were taken for **(E)** the total distance traveled, **(F)** the percentage of time spent in
526 the correct quadrant, and **(G)** the number of times crossing the boundary of the platform. A week
527 after the first probe trial, mice were again tested with a second probe trial and measurements were
528 taken for the number of times crossing the boundary of the platform **(H)**. Data shown are mean +
529 SEM, $*P < 0.05$, $**P < 0.01$, $n = 7$ and 7 for saline and DCA treatments, respectively.

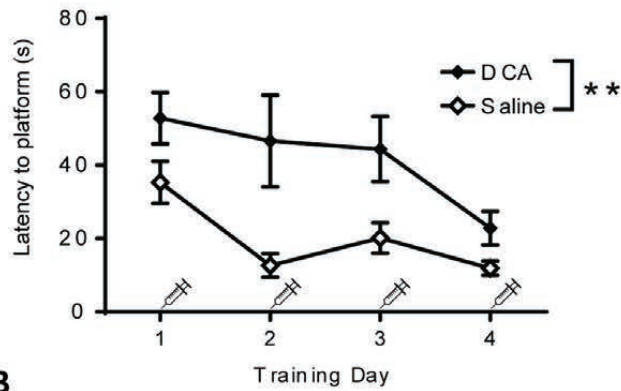
530

531 **Figure 4. DCA administration does not interfere with memory retrieval.** MWM performed by
532 mice i.p. injected with saline or DCA (200mg/kg) on the probe trial. (A) Mice were trained for 4
533 consecutive days (4 trials per day) to find the location of a hidden platform in the SW quadrant
534 and the latency to escape was recorded. On day 5, a probe trial was performed in which the
535 platform was removed and mice were allowed to swim for 60 seconds (B-G). (B) The swim path
536 for each group of mice was recorded and compiled into heat map representations. Measurements
537 were taken for (C) the total distance traveled, (D) the percentage of time spent in the correct
538 quadrant, and (E) the number of times crossing the boundary of the platform. Immediately after
539 the probe trial, a flag trial was performed and the latency to find the flag was recorded (F). Data
540 shown are mean + SEM, n = 9 and 10 for saline and DCA treatments, respectively. No significant
541 differences were observed between saline- (sham) and DCA-injected mice.
542

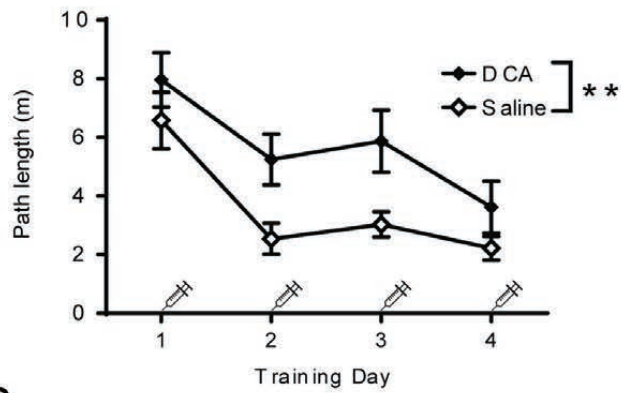




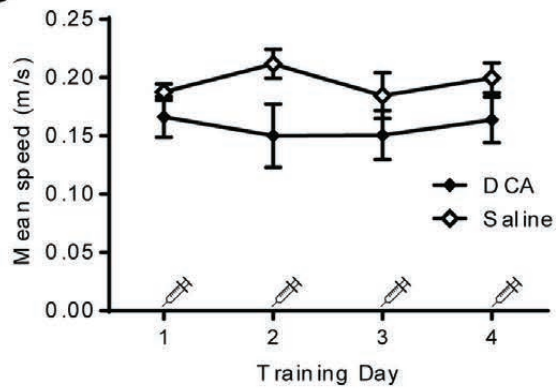
A



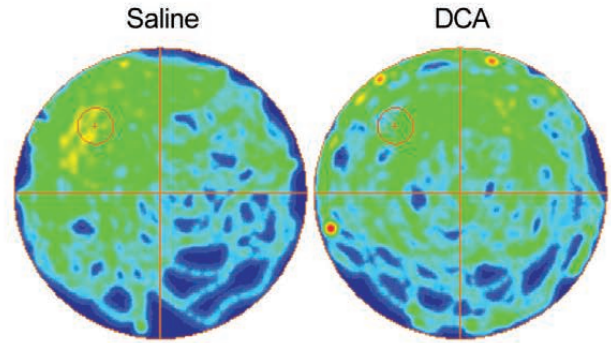
B



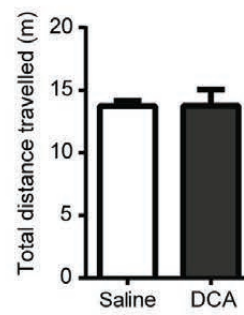
C



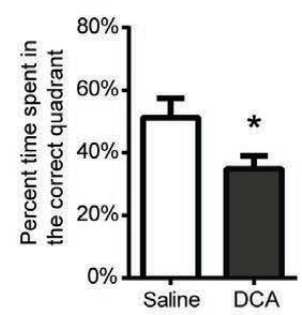
D



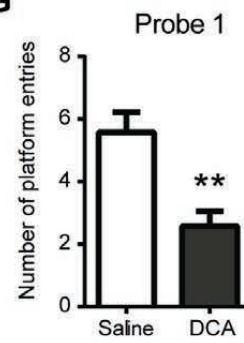
E



F



G



H

